Plasma Response to Externally Applied Resonant Magnetic Perturbations

Q. Yu and S. Günter

Max-Planck-Institut für Plasmaphysik, EURATOM Association, D-85748 Germany
email: qiy@ipp.mpg.de

The response of tokamak plasmas to applied resonant magnetic perturbations (RMPs) is studied numerically by using the nonlinear two-fluid equations. It is found that either the plasma rotation frequency or the local electron temperature and density gradient (diamagnetic drift frequency) can be significantly changed by RMPs. Depending on plasma parameters, the RMP amplitude and the original equilibrium plasma rotation direction and frequency, the RMP can either speed up or slow down plasma rotation or even change the rotation direction. Similarly, the RMP can either increase or decrease the local electron density gradient. The electron temperature changes in a different way from the electron density due to the parallel heat diffusion. The particle transport in stochastic magnetic fields is found to be similar to that across a single magnetic island.

1. Introduction

Resonant magnetic perturbations (RMPs) are of increasing importance for tokamak plasmas. In addition to intrinsic machine error fields and fields generated by mirror currents in the walls, actively applied RMPs are being used to influence plasma stability. The following issues are of particular concern for a fusion reactor:

(a) **Mode locking**: The locking of large magnetic islands by error fields or applied RMPs is often observed in tokamak experiments, leading to severe confinement degradation or even to disruptions [1-3]. The mode locking threshold is found to be proportional to the plasma viscosity and the mode frequency but inversely proportional to the square of the magnetic island width and the Alfven velocity, indicating that low-m NTMs will be much more easily locked by the error field in a fusion reactor than in existing tokamaks [4].

(b) **Mitigation of Edge Localized Modes** (ELMs): An appropriate amplitude of RMPs is found to be able to control ELMs while maintaining the H-mode pedestal [5].

(c) **Error field penetration**: Experimental results indicate that the penetration threshold has a minimum when the applied helical field frequency is the same as the mode frequency being determined by both the plasma rotation and the diamagnetic drift. As the field frequency deviates from the mode frequency, the threshold significantly increases and is asymmetric on the two sides of the minimum [6]. The nonlinear numerical results based on two fluids equations agree with the experimental observations [7].

There were many theoretical studies on the plasma response to RMPs based on (reduced) MHD equations [2,8] Some phenomena observed in experiments, such as the increased bulk plasma rotation or the change of the plasma rotation from the electron diamagnetic drift direction into the ion's direction by an applied static RMP [2,9], can not be explained in this framework. Applied RMPs degrade tokamak particle confinement in many experiments, while improved confinement by RMPs was observed in others [2,10], a phenomenon contradicting the conventional understanding that magnetic islands generated by RMPs would flatten the local plasma density profile. For a better understanding of the experimental results, the plasma response to applied RMPs is studied numerically by using the nonlinear two-fluid equations.

2. Theoretical model and quasilinear results

The large aspect-ratio tokamak approximation is utilized. The magnetic field is defined as $B=B_{0t}-(kr/m)B_{0t}\mathbf{e}_\theta+\nabla\psi\times\mathbf{e}_t$, where ψ is the helical flux function, m/r and k=n/R are the wave vectors in $\mathbf{e}_\theta$ (poloidal) and $\mathbf{e}_t$ (toroidal) direction, respectively, R is the major radius, and the subscript 0 denotes an equilibrium quantity. The ion velocity $v=v_\parallel\mathbf{e}_\parallel+\mathbf{v}_\perp$, where $v_\parallel$ and $\mathbf{v}_\perp=\nabla\phi\times\mathbf{e}_t$ are the parallel (to the magnetic field) and the perpendicular velocity, respectively. The cold ion assumption is made.

To obtain ψ, $v_\parallel$, $\mathbf{v}_\perp$, the electron density n_e and temperature T_e, the electron continuity equation, the generalized Ohm's law, the equation of motion in the parallel and the perpendicular direction (after taking the operator $\mathbf{e}_t\cdot\nabla\times$), and the electron energy transport equation, are solved [11]. Normalizing the length to the minor radius a, the time t to τ_R, ψ to aB_{0t}, $\mathbf{v}$ to a/τ_R, and T_e and n_e to their values at the magnetic axis, where a is the minor radius, and $\tau_R=a^2/\eta$ is the resistive time, these equations become

$$\frac{dn_e}{dt}=d_1\nabla_\parallel j-\nabla_\parallel(n_e v_\parallel)+\nabla\cdot(D_\perp\nabla n_e)+S_n\,, \tag{1}$$

$$\frac{d\psi}{dt}=E-\eta j+\Omega(\nabla_\parallel n_e+\nabla_\parallel T_e)\,, \tag{2}$$

$$\frac{dv_\parallel}{dt}=-C_s^2\nabla_\parallel P/n_e+\mu\nabla_\perp^2 v_\parallel\,, \tag{3}$$

$$\frac{dU}{dt}=-S^2\nabla_\parallel j+\mu\nabla_\perp^2 U+S_m\,, \tag{4}$$

$$\frac{3}{2}n_e\frac{dT_e}{dt}=d_1T_e\nabla_\parallel j-T_e n_e\nabla_\parallel v_\parallel+n_e\nabla\cdot(\chi_\parallel\nabla_\parallel T_e)+n_e\nabla\cdot(\chi_\perp\nabla_\perp T_e)+S_p\,, \tag{5}$$

where $d/dt=\partial/\partial t+\mathbf{v}_\perp\cdot\nabla$, j is the plasma current density along the $\mathbf{e}_t$ direction, $U=-\nabla_\perp^2\phi$ is the plasma vorticity, μ the plasma viscosity, χ the heat conductivity, and D the particle diffusivity. $P=n_eT_e$, and the subscripts $\parallel$ and $\perp$ denote the parallel and the perpendicular components, respectively. S_n, S_p and E are the particle and heat source and the equilibrium electric field, respectively. S_m is the poloidal momentum source which leads to an equilibrium poloidal plasma rotation. The parameters in Eqs. (1)-(5) are given by $d_1=\omega_{ce}/\nu_e$, $\Omega=\beta_e d_1$, $C_s=[T_e/m_i]^{1/2}/(a/\tau_R)$, and $S=\tau_R/\tau_A$, where $\beta_e=4\pi n_eT_e/B_{0t}^2$, ω_{ce} and ν_e are the electron cyclotron and the collisional frequency, and $\tau_A=a/V_A$ is the toroidal Alfven time.

The mechanism affecting the particle confinement by a RMP has been demonstrated by quasi-linear analysis [12]. When the amplitude of the RMP is sufficiently small, the $\mathbf{v}_\perp\cdot\nabla n_e$ and $\nabla_\parallel(n_ev_\parallel)$ terms in Eq. (1) can be neglected, and the balance between the $\nabla_\parallel j$ term and the perpendicular transport leads to [12]

$$r_s(\Delta n_e)'/n_e=d_1(\omega_{*e0}r_s^2/D_\perp)(1-\omega_0)|b_{1r}/B_{0t}|^2/m \tag{6}$$

at $r=r_s$ in steady state for a static RMP, where $\Delta n_e=(n_{e,0/0}-n_{e0})$, $n_{e,0/0}$ is the m/n=0/0 component of n_e, n_{e0} is the original equilibrium electron density, r_s is the minor radius of the rational surface, and b_{1r} is the radial magnetic field perturbation.

$$\omega_0\equiv-\omega_{E0}/\omega_{*e0}$$

is the ratio between the equilibrium plasma rotation frequency and the electron diamagnetic drift frequency. $\omega_0>0$ refers to the plasma rotation in the ion drift direction (plasma current direction for a toroidal rotation). Eq. (6) indicates that the electron density gradient is decreased by a RMP of a single helicity ($|n_e'/n_e|$ increases in the standard case where the equilibrium density gradient is negative) for $\omega_0>1$, while in the opposite case $(\Delta n_e)'>0$. The $\nabla_\parallel j$ term in Eq. (5) drives a similar change in the electron temperature gradient, but the parallel heat diffusion tends to flatten the local electron temperature profile.

In addition, the electromagnetic torque due to the applied RMP drives the plasma rotation frequency ω_E to approach the negative electron diamagnetic drift frequency, $-\omega_{*e}$. Assuming that the viscous force is larger than the plasma inertia, one finds [12,13]

$$\Delta\omega/\omega_{E0} \approx (\tau_R V_A^2/\mu)[(w/a)(r/R)/q]^2(1/\omega_0-1)|b_{1r}/B_{0t}|^2 \qquad (7)$$

for a toroidal plasma rotation with $\Delta\omega \ll \omega_{E0}$, where $\Delta\omega=(\omega_E-\omega_{E0})$, ω_{E0} is the equilibrium plasma rotation frequency, $w=4[(b_{1r}Rq)/(B_{0t}nq')]^{1/2}$ is the magnetic island width under the constant ψ assumption, and q is the safety factor. Eq. (6) predicts a significant change in the electron density gradient only under the condition

$$(\Delta\omega/\omega_{E0})/[(\Delta n_e)'/(n_e/r)] \ll 1. \qquad (8)$$

In the opposite limit of (8), RMPs lead to $\omega_E \approx -\omega_{*e} \approx -\omega_{*e0}$ before a significant change in the electron density [12,13], and the ω_{*e0} and the $(1-\omega_0)$ terms in Eq. (6) should be replaced by ω_{*e} and $(1+\omega_E/\omega_{*e})$, respectively, if ω_E and ω_{*e} are significantly different from ω_{E0} and ω_{*e0}.

3. Numerical results for a single helicity RMP

Eqs (1)-(5) are solved simultaneously using the initial value code TM1, which has been used earlier for modelling drift tearing modes [11]. A single helicity RMP with m/n=2/1 is taken into account by the boundary condition

$$\psi_{2/1}|_{r=a} = \psi_a a B_{0t} cos(m\theta+n\phi), \qquad (9)$$

where ψ_a describes the normalized m/n=2/1 helical magnetic flux amplitude at r=a. The input parameters are based on TEXTOR experimental parameters. A monotonic q profile is used with the q=2 surface located at r_s=0.628a [9]. The m/n=2/1 tearing mode is stable for ψ_a=0. The toroidal magnetic field is B_{0t}=2.5T, the plasma minor and major radius are a=0.47m and R=1.75m. The following parameters, $S=1.97\times10^8$, $\Omega=6.3\times10^4$, $c_s=1\times10^7(a/\tau_R)$, $d_1=2.5\times10^8$, $\chi_{\|}=10^8(a^2/\tau_R)$, $\chi_\perp=D_\perp=14(a^2/\tau_R)$ and $\mu=2.1\times10^3(a^2/\tau_R)$ are used in the calculations except mentioned elsewhere. In TEXTOR experiments the plasma rotation is essentially toroidal [9], while in Eqs. (1)-(5) due to large aspect ratio approximation only a poloidal rotation is included, so that a larger plasma viscosity is used in our calculations for a reasonable balance between the electromagnetic and the viscous force.

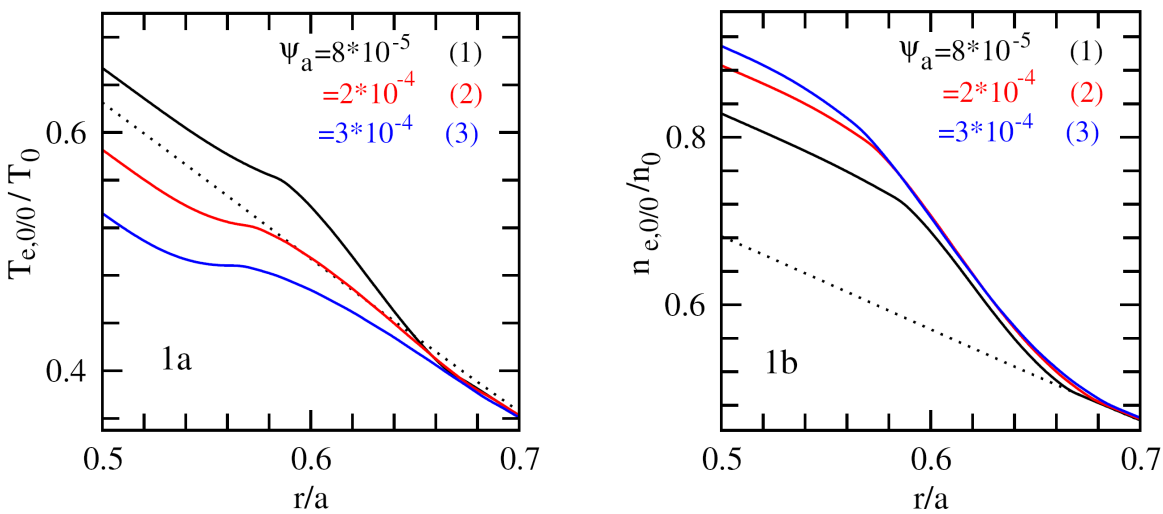

Fig. 1: Effect of the RMP amplitude on radial profiles of the (normalized) m/n=0/0 component of electron temperature (left, 1a) and density (right, 1b). The dotted curves show the radial profiles of the original equilibrium electron temperature and density. The equilibrium plasma rotation is in the ion drift direction with ω_0=2.97.

The radial profiles of the (normalized) m/n=0/0 component of the electron temperature, $T_{e,0/0}/T_0$, in steady state are shown by the solid curves in Fig. 1a for ω_0=2.97 with $\psi_a=8\times10^{-5}$, 2×10^{-4} and 3×10^{-4}, where T_0 is the equilibrium electron temperature at r=0. The corresponding magnetic island widths are w/a=0.0857, 0.116 and 0.126, respectively. The dotted curve shows the radial profile of the original equilibrium electron temperature. The electron temperature increases across the rational surface for $\psi_a=8\times10^{-5}$, forming a kind of pedestal there as expected for a constant perpendicular heat diffusivity. For larger ψ_a, the electron temperature decreases, because the parallel heat diffusion is more important for a larger magnetic island. Corresponding to Fig. 1a, radial profiles of the (normalized) m/n=0/0 component of the electron density, $n_{e,0/0}/n_0$, in steady state are shown by the solid curves in Fig. 1b, where n_0 is the equilibrium electron density at r=0. The dotted curve shows the equilibrium electron density profile. The local electron density increases more significantly for a larger value of ψ_a.

For the plasma rotation in the electron drift direction with ω_0=-1.98, radial profiles of $T_{e,0/0}/T_0$ in steady state are shown in figure 2a with $\psi_a=8\times10^{-5}$, 10^{-4} and 3×10^{-4}. The corresponding island widths are w/a=0.0125, 0.0884 and 0.130, respectively. The dotted curve shows again the equilibrium electron temperature profile. With increasing ψ_a, the electron temperature first decreases, and the local temperature gradient changes from the usual negative value to a positive one. For sufficiently large ψ_a, the temperature profile flattens because of the parallel heat diffusion. Corresponding to Fig. 2a, radial profiles of $n_{e,0/0}/n_0$ are shown in Fig. 2b. The electron density decreases more significantly across the rational surface for a larger value of ψ_a.

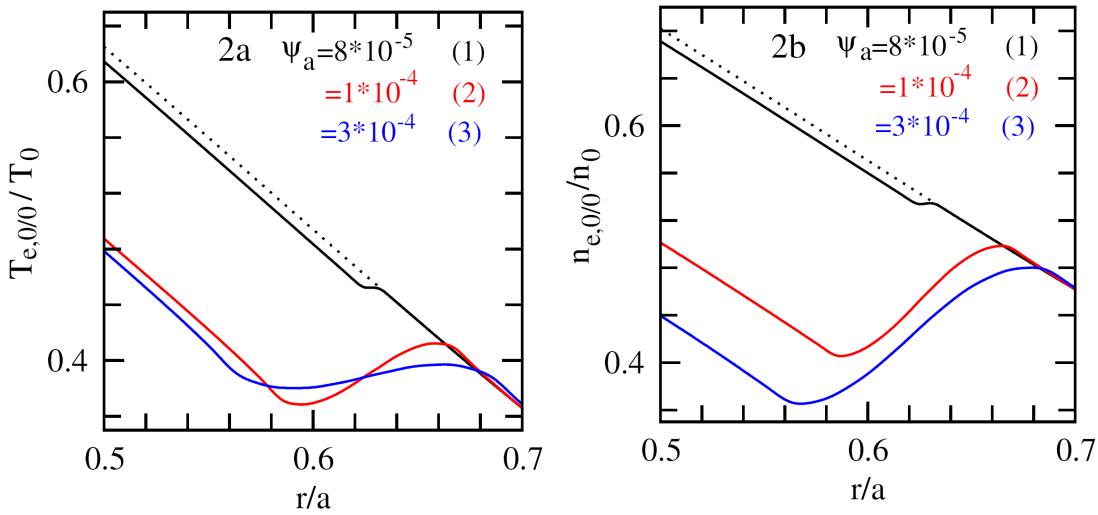

Fig. 2: Radial profiles of the (normalized) m/n=0/0 component of electron temperature (left, 2a) and density (right, 2b) . The original equilibrium plasma rotation is in the electron drift direction with ω_0=-1.98.

The effect of the parallel heat diffusion on electron temperature profile is shown in figure 3a for ω_0=-1.98 and $\psi_a=10^{-4}$, with $\chi_{||}=10^7$, 10^8 and 1.6×10^9. The corresponding island widths are w/a=0.0886, 0.0884, 0.0859, respectively. With increasing $\chi_{||}$, the temperature profile becomes more flattened. The corresponding electron density (Fig. 3b) decreases more significantly across the rational surface for a larger $\chi_{||}$ with the flattening of the local temperature profile.

For the plasma rotation in the ion drift direction with ω_0=2.97, the electron temperature

profiles in steady state are shown in figure 4a for $\psi_a = 8\times10^{-5}$, with $\chi_{\|}=10^7$, 10^8 and 10^9. The corresponding island widths are w/a=0.0877, 0.0858 and 0.0823, respectively. The local temperature increases for $\chi_{\|}$ up to 10^8 but decreases for $\chi_{\|}=10^9$. The corresponding electron density (Fig. 4b) increases more significantly across the rational surface for a lager $\chi_{\|}$.

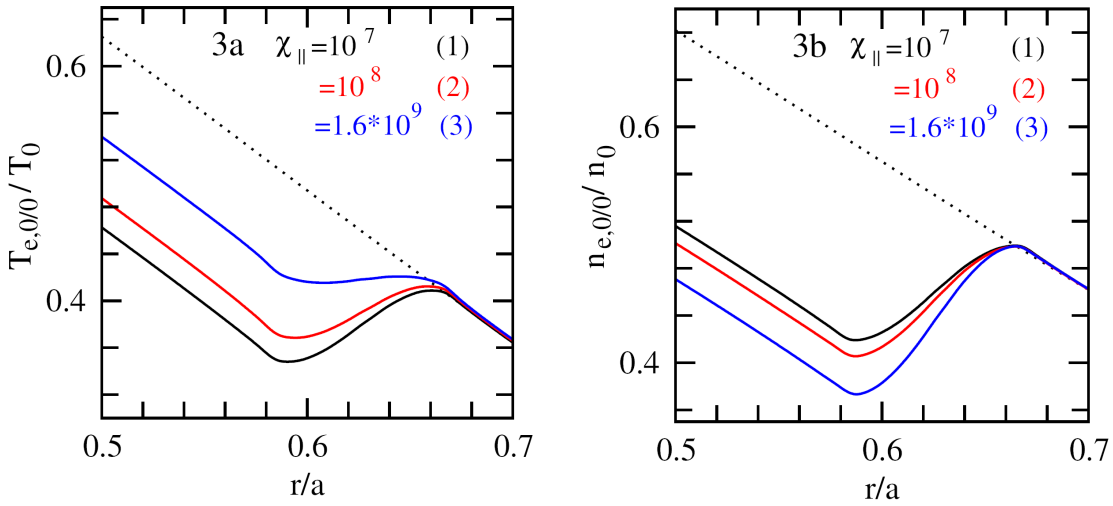

Fig. 3: Effect of parallel heat diffusion on radial profiles of the m/n=0/0 component of electron temperature (left, 3a) and density (right, 3b). The original equilibrium plasma rotation is in the electron drift direction with ω_0=-1.98.

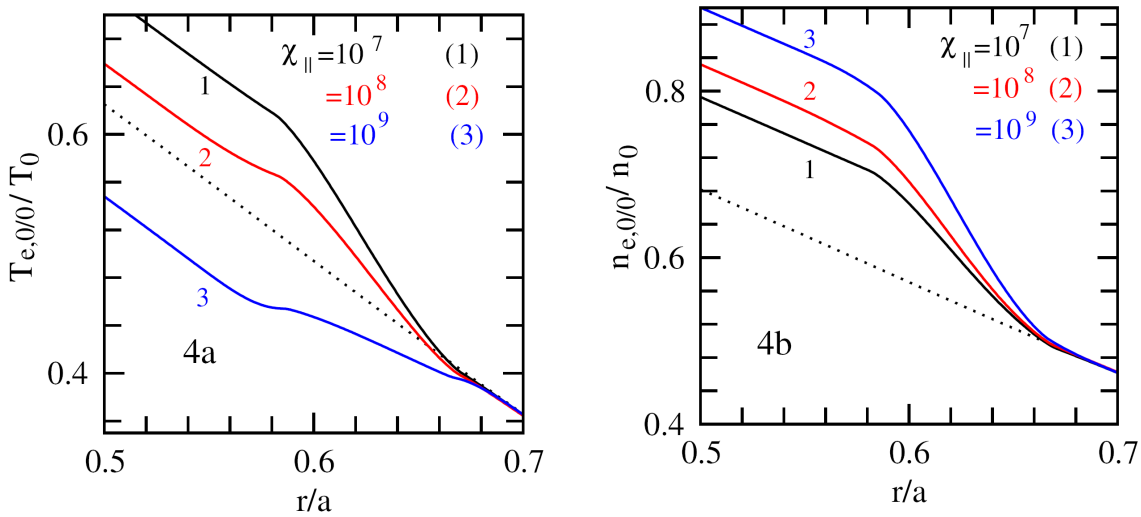

Fig. 4: Radial profiles of the m/n=0/0 component of electron temperature (left, 4a) and density (right, 4b). The original equilibrium plasma rotates in the ion drift direction with ω_0=2.97.

It is seen from Figs. 1-4 that the change of the local gradient of the electron temperature and density by RMPs is coupled. The flattening in the local electron temperature profile due to a larger value of $\chi_{\|}$ or island width enhances the change of the electron density gradient. The effect of other parameters on the electron temperature and density profiles has also been studied. The local electron temperature and density gradient is changed more by the RMP for a larger value of d_1, $|\omega_0-1|$ or smaller perpendicular heat and particle diffusivity, as predicted by the analytical theory [12,13].

In the above results the change of the plasma rotation frequency is not significant. The effect of RMPs on plasma rotation is determined by the balance between the electromagnetic and viscous torque, which is affected by the parameter $S^2/(\mu\tau_R/a^2)$ as seen from Eq. (4). A larger value of $S^2/(\mu\tau_R/a^2)$ leads to a bigger change in plasma rotation.

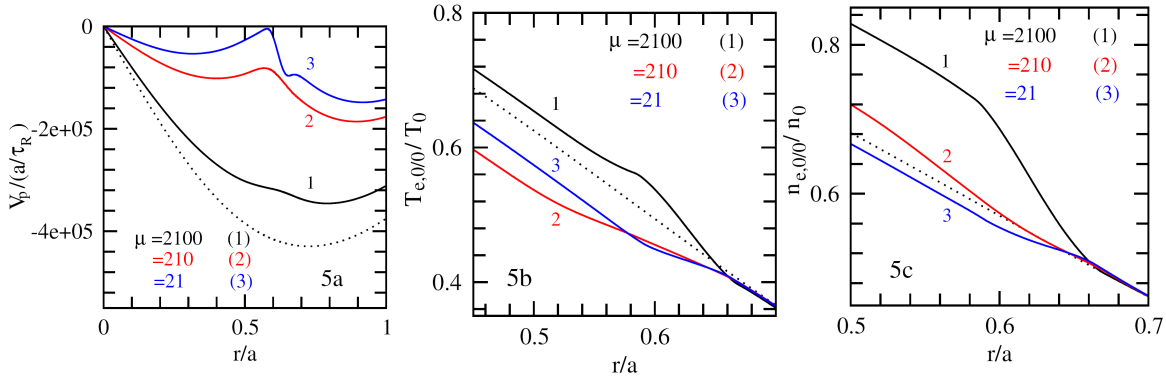

Fig. 5: Radial profiles of the (normalized) m/n=0/0 component of poloidal plasma rotation velocity (left, 5a), electron temperature (middle, 5b) and density (right, 5c). The equilibrium plasma rotates in the ion drift direction with ω_0=2.97.

The (normalized) m/n=0/0 component of the poloidal plasma rotation velocity, V_p, is shown in figure 5a for ω_0=2.97 and $\psi_a=8\times10^{-5}$, with μ=2100, 210 and 21(a^2/τ_R). The corresponding island widths are w/a=0.0857, 0.0871 and 0.0740, respectively. The dotted curve shows the original poloidal velocity profile unperturbed by the RMP. With decreasing μ, the plasma rotation velocity decreases more. Corresponding to Fig. 5a, radial profiles of $T_{e,0/0}/T_0$ and $n_{e,0/0}/n_0$ are shown in Fig. 5b and 5c. The electron temperature and density decrease across the rational surface for a sufficiently small μ.

For the plasma rotation in the electron drift direction with ω_0=-1.98, radial profiles of V_p are shown in figure 6a with $\psi_a=10^{-4}$ for μ=2100, 210 and 21(a^2/τ_R). The corresponding island widths are w/a=0.0857, 0.0871 and 0.0740, respectively. With decreasing μ, the plasma rotation velocity first decreases and then changes its direction from the electron drift direction to the ion's direction around the rational surface. The corresponding radial profiles of $T_{e,0/0}/T_0$ and $n_{e,0/0}/n_0$ are shown in Fig. 6b and 6c. The electron temperature and density decrease less across the rational surface for a smaller μ.

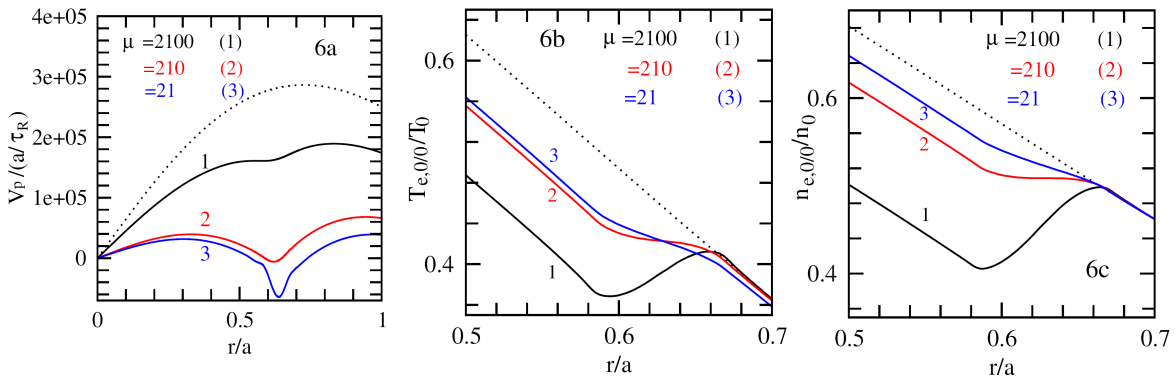

Fig. 6: Radial profiles of the (normalized) m/n=0/0 component of poloidal plasma rotation velocity (left, 6a), electron temperature (middle, 6b) and density (right, 6c). The equilibrium plasma rotates in the electron drift direction with ω_0=-1.98.

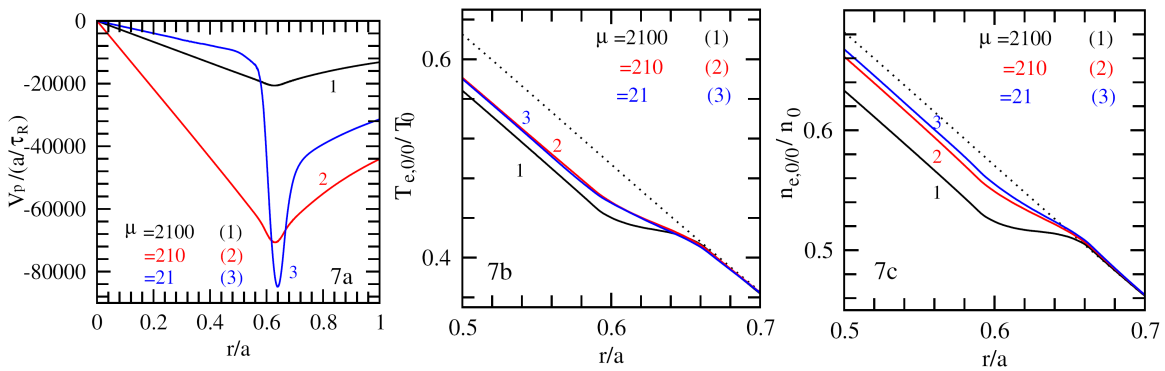

Fig. 7: Radial profiles of the (normalized) m/n=0/0 component of poloidal plasma rotation velocity (left, 7a), electron temperature (middle, 7b) and density (right, 7c). The original equilibrium plasma rotation speed is zero.

For zero equilibrium plasma rotation, the radial profiles of V_p in steady state are shown in figure 7a with $\psi_a=8\times10^{-5}$ for μ=2100, 210 and 21(a^2/τ_R). The corresponding island widths are w/a=0.0756, 0.0765 and 0.0748. The RMP drives the plasma to rotate in the ion drift direction, in agreement with the experimental observations [9]. With decreasing μ, the plasma rotation velocity increases more. Corresponding to Fig. 7a, radial profiles of $T_{e,0/0}/T_0$ and $n_{e,0/0}/n_0$ are shown in Fig. 7b and 7c. The electron temperature and density decrease less across the rational surface for a smaller μ. It is seen from Figs. 5-7 that a larger change in the plasma rotation velocity corresponds to a smaller change in the local electron temperature and density gradient.

4. Particle transport across a local stochastic magnetic field

The local magnetic field becomes stochastic when islands of different helicity overlap. An applied m/n=9/5 RMP is further introduced in our calculation in addition to the m/n=2/1 RMP, with the q=9/5 surface at r_s=0.593a, being close to the q=2 surface.

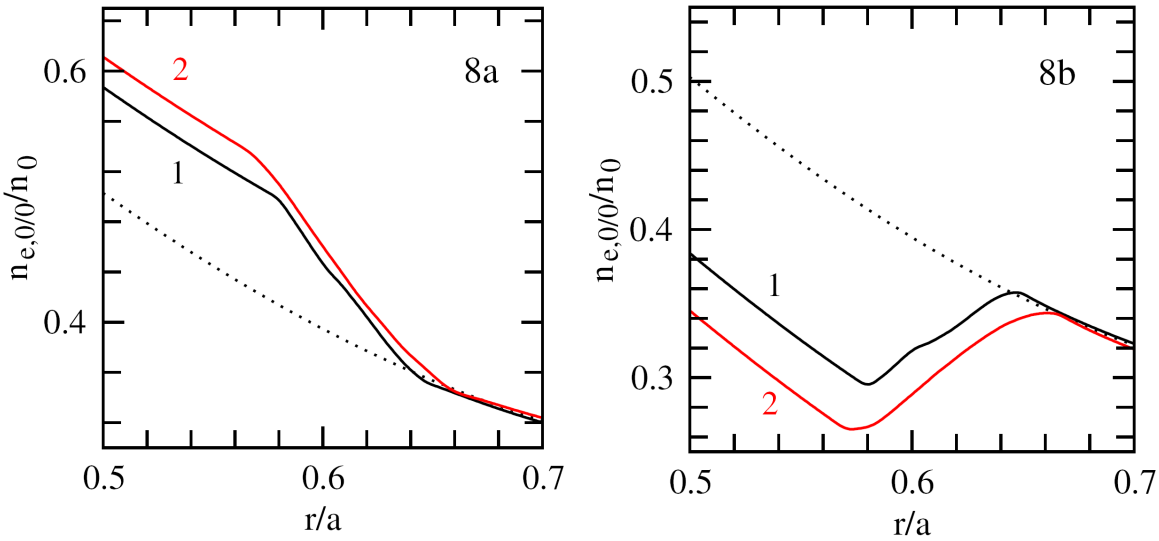

Fig. 8 Radial profiles of the m/n=0/0 component of electron density for original plasma rotation in the ion drift direction (left, 8a, ω_0=2.92) and in the electron's direction (right, 8b, ω_0=-1.62) .

In the following results the electron temperature perturbations are neglected, and only the particle transport is calculated by using Eqs. (1)-(4) due to computational limitation. In Fig. 8a radial profiles of $n_{e,0/0}/n_0$ in steady state are shown for ω_0=2.92 with (1) $\psi_{a,2/1}$= 1.8×10^{-5} and $\psi_{a,9/5}=8\times10^{-4}$; (2) $\psi_{a,2/1}=10^{-4}$ and $\psi_{a,9/5}=10^{-3}$. The Chirikov parameters are Δ=0.94 and 1.55, respectively, calculated only by the m/n=/2/1 and 9/5 islands. In fact, many small islands of other helicities are also excited by the applied m/n=2/1 and 9/5 RMPs. Fig. 8b are for the original equilibrium plasma rotates in the electron drift direction with ω_0=-1.62 for (1) $\psi_{a,2/1}=2\times10^{-5}$ and $\psi_{a,9/5}=9\times10^{-4}$; (2) $\psi_{a,2/1}=10^{-4}$ and $\psi_{a,9/5}=9\times10^{-4}$. The Chirikov parameters are Δ=0.981, and 1.53 respectively. The electron density increases across the rational surface for the plasma rotation in the ion drift direction but decreases in the opposite case, being similar to that caused by a single helicity RMP.

5. Summary

The plasma response to RMPs has been shown to be affected by the plasma rotation direction and frequency, the RMP amplitude, and the particle, heat and momentum transport coefficients. The major obtained results are as the following:

(1) In case of a sufficiently high value of $S^2/(\mu\tau_R/a^2)$, the change of the plasma rotation frequency is more significant than that of the local electron density and temperature gradient (or electron diamagnetic drift frequency). The RMP can either speed up or slow down the plasma rotation or even change the rotation direction, depending on the original equilibrium plasma rotation frequency and direction.

(2) In case of a sufficiently low value of $S^2/(\mu\tau_R/a^2)$, the change of the local electron density gradient can be significant, especially for plasmas with high rotation speeds, large values of d_1 or small perpendicular particle diffusivity at the resonant surface. The RMP can either increase or decrease the local electron density gradient, depending on the original equilibrium plasma rotation frequency and direction. The electron temperature changes in a similar way to the electron density, if the local parallel heat diffusivity and the island width are not too large. In the opposite limit the local electron temperature profile flattens, which enhances the change in the local electron density gradient.

(3) The particle transport in stochastic magnetic fields is found to be similar to that caused by a single helicity RMP.

Acknowledgment: Q. Yu is grateful to Dr. K. H. Finken for helpful discussions.

[1] M.F.F. Nave and J.A. Wesson, Nucl. Fusion **30**, 2575 (1990).
[2] T.C. Hender, R. Fitzpatrick, A.W. Morris *et al*, Nucl. Fusion **32**, 2091 (1992).
[3] H. Zohm, A. Kallenbach, H. Bruhns, et al, Europhys. Letts. **11**, 745 (1990).
[4] Q. Yu and S. Günter, Nucl. Fusion **48**, 065004 (2008).
[5] T.E. Evans, R.A. Moyer, P.R. Thomas, et al., Phys. Rev. Letts. **92**, 235003 (2004).
[6] H.R. Koslowski, Y. Liang A. Krämer-Flecken et al., Nucl. Fusion **46**, L1 (2006).
[7] Q. Yu, S. Günter, Y. Kikuchi, and K. H. Finken, Nuclear Fusion **48**, 024007 (2008).
[8] R. Fitzpatrick, Nucl. Fusion **33**, 1049 (1993).
[9] K.H. Finken, S.S.Abdullaev, M.F.M. De Bock *et al*, Phys. Rev. Letts **94** 015003(2005).
[10]K.H.Finken, S.S.Abdullaev, M.W.Jakubowski *et al*, Phys. Rev. Letts **98** 065001(2007).
[11] Q. Yu, Nucl. Fusion 50, 025014 (2010).
[12] Q. Yu and S. Günter, Nucl. Fusion **49**, 062001 (2009).
[13] Q. Yu, S. Günter and K.H. Finken, Phys. Plasmas **16**, 042301 (2009).